Microscopic structure of the one-phonon 2^+ states of ^{208}Po

D. Kalaydjieva,[1, a] D. Kocheva,[1, b] G. Rainovski,[1] V. Karayonchev,[2] J. Jolie,[2] N. Pietralla,[3] M. Beckers,[2] A. Blazhev,[2] A. Dewald,[2] M. Djongolov,[1] A. Esmaylzadeh,[2] C. Fransen,[2] K. A. Gladnishki,[1] A. Goldkuhle,[2] C. Henrich,[3] I. Homm,[3] K. E. Ide,[3] P. R. John,[3] R. Kern,[3] J. Kleemann,[3] Th. Kröll,[3] C. Müller-Gatermann,[2, c] M. Scheck,[4] P. Spagnoletti,[4] M. Stoyanova,[1] K. Stoychev,[1] V. Werner,[3] A. Yaneva,[1, 2] S. S. Dimitrova,[5] G. De Gregorio,[6, 7] H. Naïdja,[8] and A. Gargano[7]

[1] *Faculty of Physics, St. Kliment Ohridski University of Sofia, 1164 Sofia, Bulgaria*
[2] *Institut für Kernphysik, Universität zu Köln, 50937 Cologne, Germany*
[3] *Institut für Kernphysik, Technische Universität Darmstadt, 64289 Darmstadt, Germany*
[4] *CEPS, University of the West of Scotland, PA1 2BE Paisley, UK and SUPA, Glasgow G12 8QQ, UK*
[5] *Institute for Nuclear Research and Nuclear Energy, Bulgarian Academy of Sciences, 1784 Sofia, Bulgaria*
[6] *Dipartimento di Matematica e Fisica, Università degli Studi della Campania "Luigi Vanvitelli", I-81100 Caserta, Italy*
[7] *INFN Sezione di Napoli, IT-80126 Napoli, Italy*
[8] *Université Constantine 1, Laboratoire de Physique Mathématique et Subatomique (LPMS), Constantine 25000, Algeria*

(Dated: July 7, 2021)

The lifetimes of the 2_1^+ and 4_1^+ states of ^{208}Po were measured in the α-transfer reaction ^{204}Pb(^{12}C,^{8}Be)^{208}Po by γ-ray spectroscopy utilizing the recoil distance Doppler Shift method. The newly extracted transition strengths alongside with ones of the decay of 2_2^+ state were compared to the results of large-scale shell-model calculations using an effective interaction derived from the realistic CD-Bonn nucleon-nucleon potential. The comparison indicates the importance of the quadrupole isovector excitations in the valence shell for a fine tuning of the two-body matrix elements of the shell-model interaction.

I. INTRODUCTION AND MOTIVATION

The atomic nucleus as a two-fluid many-body quantum system provides an unique laboratory for studying different quantum phenomena. Among them the appearance and the different forms of manifestation of nuclear quadrupole collectivity still attract significant interest. This is particularly true for collective states in even-even nuclei in the vicinity of double magic nuclei, where the relatively small number of valence particles (holes) allows a description of their low-lying collective states in the shell-model framework [1, 2]. The comparison of shell-model results with experimental data reveals the microscopic structure of these states and allows to identify and, eventually, adjust the two-body matrix elements of the effective shell-model interaction which give rise to the configuration mixing responsible for the observed properties of the collective states.

In general, collective excitations can be considered as a coherent movement of valence nucleons caused by the residual interaction, dominated by the proton-neutron interaction [4]. One of the simplest manifestations of these excitations in weakly-collective open-shell even-even nuclei are the one-phonon 2^+ vibrational states. Due to the two-fluid nature of the nuclear matter they appear as a symmetric [the one-phonon 2_1^+ fully symmetric state (FSS)] or an antisymmetric [the so called mixed symmetry state (MSS), $2_{1,ms}^+$] combination of the involved proton and neutron configurations [5]. These two distinct forms of one-phonon 2^+ states are built on identical configurations, the only difference being the relative sign between the involved proton and neutron configurations. The MSSs may provide good probe to investigate the components of the effective proton-neutron interaction which lead to the formation of collective isovector excitations.

Because of their isovector nature the one-phonon $2_{1,ms}^+$ state decays with a strong $M1$ transition to the 2_1^+ state and with a weak $E2$ transition to the ground state. This unique decay serves as a signature for experimental identification of the one-phonon $2_{1,ms}^+$ states [6]. Such states have been observed throughout the table of isotopes, and the best examples of one-phonon MSSs are found in the mass $A \approx 90$ region [6, 7]. Several MSSs are also present in the mass $A \approx 130$ region [6, 8–13]. Recently, a few examples of MSSs have been found in weakly collective nuclei around the doubly-magic core ^{208}Pb [14–17].

Although the experimental data for one-phonon MSSs are relatively abundant, a limited number of attempts to understand their electromagnetic properties in terms of microscopic models is available. Calculations are usually carried out either in the framework of the Quasiparticle-phonon model [18] or in the framework of the nuclear shell model [19]. There are several studies of one-phonon MSSs in the mass $A \approx 90$ and $A \approx 130$ regions within the realistic shell-model [11, 20–24]. For $A \approx 208$ the one-phonon MSS of ^{212}Po is described in the framework of a single-j shell model calculations [14] as it has been shown that the isovector character of the $2_{1,ms}^+$ of ^{212}Po

[a] Present address: IRFU, CEA, Université Paris-Saclay, F-91191 Gif-sur-Yvette, France
[b] Corresponding author: dkocheva@phys.uni-sofia.bg
[c] Present address: Argonne National Laboratory, 9700 South Cass Ave, Argonne, IL 60439, United States

appears solely from the leading single-particle valence shell configuration. In this respect, the relatively low $B(M1; 2^+_{1,ms} \rightarrow 2^+_1)$, compared to the ones in the cases of single-isolated MSSs, observed in ^{212}Po [14] can be attributed to the low quadrupole collectivity in this nucleus [25]. In ^{208}Po which is the neutron particle-hole mirror of ^{212}Po, a similar low $B(M1)$ strength between the 2^+_2 and the 2^+_1 states has been observed [17]. On this basis the 2^+_2 state of ^{208}Po has been assumed to be a fragment of the one-phonon mixed-symmetry state. However, as has been noted in Ref.[17], experimental data on the $B(E2; 2^+_1 \rightarrow 0^+_1)$ state and detailed shell-model calculations are needed to confirm this conjecture. To infer the isovector nature of the 2^+_2 state of ^{208}Po based on shell-model calculations it is necessary to demonstrate that the calculations are capable of reproducing, at least qualitatively, the electromagnetic properties of both 2^+_1 and the 2^+_2 states of ^{208}Po. Up to know the experimental lifetime of the 2^+_1 state of ^{208}Po is not known. In the present study, we report the first experimental measurement on the lifetime of the 2^+_1 state of ^{208}Po, as well as results from large-scale shell-model calculations which reveal a significant isovector component in the structure of the 2^+_2 state of ^{208}Po.

II. EXPERIMENTAL SETUP

The experiment was performed at the FN Tandem facility of the University of Cologne. The mean lifetime of the 2^+_1 state of ^{208}Po was measured by utilizing the recoil distance Doppler Shift (RDDS) method [26, 27]. The excited states of ^{208}Po were populated using the α-transfer reaction ^{204}Pb(^{12}C,^{8}Be)^{208}Po at a beam energy of 62 MeV. The target consisted of a 0.6 mg/cm^2 thin layer of ^{204}Pb (99.94% I. E.) evaporated on a 1.5 mg/cm^2 thick Ta backing foil and was placed with the Ta foil facing the beam. The stopper was a self-supporting 5.8 mg/cm^2 thick Ta foil. Data were taken at seven plunger distances: 19(3)μm, 34(3)μm, 57(3)μm, 91(3)μm, 115(3)μm, 208(4)μm and 309(4)μm. The reaction was induced inside the chamber of the Cologne plunger device [28] in which an array of solar cells was mounted. The solar cells were positioned at backward angles with respect to the beam direction. The solar cell array consisted of six 10 mm $\times$ 10 mm cells placed at a distance of about 15 mm between their centres and the target covering an angular range between 115° and 165°. The solar cells were used to detect the recoiling light reaction fragments. ^{8}Be decays immediately after the reaction to two α-particles. In order to detect these α-particles while stopping the heavier fragments from other transfer reaction channels, an Al foil with a thickness of 80 μm was placed between the target and the solar cells. The γ rays from the decay of the excited states of ^{208}Po were registered by eleven high purity germanium (HPGe) detectors mounted outside the plunger chamber in two rings at an average distance of 12 cm from the target. Five detectors were positioned at 142° with respect to the beam direction and the other six detectors were placed at 45° with respect to the beam direction.

III. DATA ANALYSIS AND RESULTS

The data were sorted offline in coincidences of at least one solar cell and one HPGe detector (particle-γ). Overall 14 particle-γ matrices were sorted depending on the positions of the HPGe detectors and the plunger distances. A projection on the particle axis of the particle-γ matrix obtained with γ-ray detection at 142° at a plunger distance of 34 μm is shown in Fig. 1(a) as an example. The γ rays in coincidence with the group of particles labeled as "^{208}Po, ^{185}Re" (the blue dashed box) in Fig. 1(a) are shown in Fig. 1(b). In this spectrum only a few transitions from excited states of the nucleus ^{185}Re are observed. This nucleus is produced by the α-transfer reaction ^{181}Ta(^{12}C,^{8}Be)^{185}Re in the backing and/or in the stopper. However, the spectrum in Fig. 1(b) is dominated by the 686- and 660-keV lines, which are the γ-ray transitions depopulating the first two excited yrast states of ^{208}Po [29]. Moreover, both transitions have well pronounced Doppler-shifted components which evolve as a function of plunger distance, see Fig. 2. This figure shows particle-gated γ-ray spectra of the $2^+_1 \rightarrow 0^+_1$ (686-keV) and $4^+_1 \rightarrow 2^+_1$ (660-keV) transitions observed at backward (a) and forward (b) angles at three different distances. The increase of the intensities of the shifted components with increasing target-to-stopper distance is apparent for both transitions and allows the determination of the lifetimes of the 2^+_1 and 4^+_1 states of ^{208}Po.

The lifetime analysis was performed with the Differential Decay Curve Method (DDCM) [30, 31]. According to this method the intensities of the shifted (I_{sh}) and unshifted (I_{un}) components (for each distance) have to be measured from spectra in coincidence with Doppler-shifted components of transitions which feed directly the state of interest. Then the lifetime τ_i of the level of interest for the i-th plunger distance can be calculated via [30, 31]:

$$\tau_i(x) = \frac{I_{un}(x)}{\langle v \rangle \frac{d}{dx} I_{sh}(x)}. \quad (1)$$

In the present analysis the determination of the lifetime by Eq. 1 is obtained by the program Napatau [32], which fits the intensity of the shifted components and calculates over separate intervals the time derivative of that curve. The trend of the time-derivative is then adapted to the trend of the unshifted peak intensities. This application of DDCM requires analyzing particle-γ-γ data for the present experiment which is not possible at the collected level of statistics. However, the particular feeding pattern of the 2^+_1 and 4^+_1 states of ^{208}Po allows this problem to be circumvented as described below.

The presented particle-gated γ-ray spectra are, in fact, singles spectra. Such spectra contain principally infor-

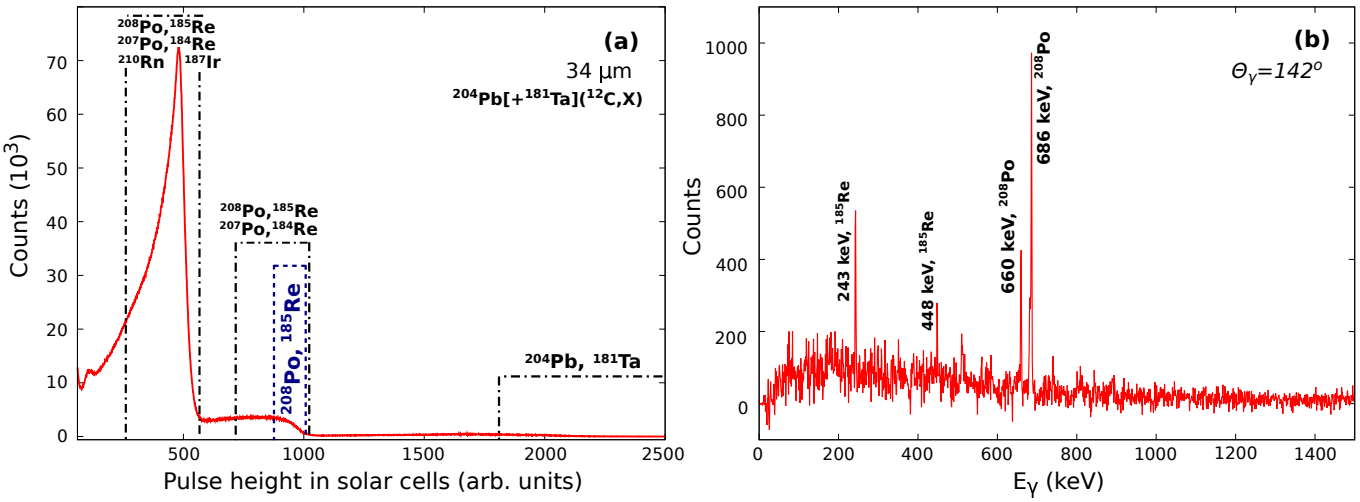

FIG. 1. (Color online) (a) The projection of the particle-γ matrix obtained at plunger distance (D=34 μm) by coincident detection of charged particles in the solar-cell array and γ rays at a polar angle $\Theta_\gamma = 142°$. The marked ranges represent parts of the particle spectrum found to be in coincidence with the γ rays from the indicated nuclei. (b) The γ-ray spectrum in coincidence with the group of particles labeled as "^{208}Po, ^{185}Re" in panel (a).

mation for the so-called effective lifetime of the state of interest. The effective lifetime aggregates the mean lifetime of the state and the partial lifetimes of all states decaying to it. Therefore, the intensities of the I_{sh} and I_{un} components of the 686-keV ($2_1^+ \rightarrow 0_1^+$) and 660-keV ($4_1^+ \rightarrow 2_1^+$) transitions derived from the spectra in Fig. 2 have to be corrected for the effects of the transitions feeding both states. In contrast to fusion-evaporation reactions, the α-transfer reaction as a direct reaction populate only discrete states. Therefore, in the present analysis it was considered that slow feeding contributions to the effective lifetimes of excited levels of ^{208}Po can originate only from discrete decays of higher-lying states, as suggested in Ref. [33]. The partial level scheme representing transitions directly populating the 2_1^+ and 4_1^+ states of ^{208}Po is shown in Fig. 3. The depicted levels are those that have been populated in our previous study, see Ref. [17]. In the present data, however, only the most intensive transitions can clearly be observed [cf. Fig. 1(b)]. In order to estimate the relative contributions of the feeding transitions to the intensities of the 686-keV and 660-keV lines we used the data from the previous measurement [17] which has utilized also the α-transfer reaction ^{204}Pb(^{12}C,^{8}Be)^{208}Po at a beam energy of 62 MeV. As a result, we can expect similar relative population of the excited states of ^{208}Po. Indeed, the data from Ref. [17] show that 38.0(3)% from the feeding of the 2_1^+ state is coming from the $4_1^+ \rightarrow 2_1^+$ transition which is in agreement with the data from the present experiment where this feeding is determined to be 40(4)%. Since the decay of the 4_1^+ state is the only well visible feeder to the 2_1^+ in the present data, the feeding states for the states of interests are taken from Ref. [17].

Using the γ-γ and the γ-particle coincidence data from the experiment in Ref. [17] we have estimated that 66% of the feeding of the 2_1^+ state originates from the states depicted in Fig. 3 as follows: 38% from the 660-keV transition, 9% from the 897-keV transition, 8% from the 734-keV transition, 6% from the 576-keV transition, 4% from the 853-keV transition, and 1% from the 1309-keV transition. Besides these levels there is only one other state observed up to date that decays directly to the 2_1^+ state of ^{208}Po, namely the 0_2^+ state at excitation energy 1271.6 keV [29]. Because the 585.1-keV ($0_2^+ \rightarrow 2_1^+$) transition is not observed in the data from our previous study [17], the remaining 34% of the intensity of the 686-keV transition is considered to originate from a direct population of the 2_1^+ state.

The lifetimes of the 2_2^+ and 4_2^+ states of the nucleus ^{208}Po were measured in our previous study [17]. They were determined to be 1.17(14) ps and 3.4(9) ps, respectively, which means that their contribution could be accepted only as fast feeding of the 2_1^+ state. The lifetimes of the 3_1^+, 2_3^+ and $(2^-, 3^-)$ states are not known and cannot be determined from any of the available data sets. In order to simplify the discussion at this moment we assume that their lifetimes are short enough so that they decay only in flight. Under this assumption the only essential feeder to the 2_1^+ state remains the 660-keV transition, which depopulates the 4_1^+ state of ^{208}Po. As can be seen from Fig. 2, the 660-keV line has Doppler-shifted and stopped (unshifted) components. Hence, the contribution coming from the decay of the 4_1^+ state to the 2_1^+ state could not be accepted neither as fast nor as slow feeding. In order to determine correctly the intensity of the unshifted component of the 686-keV transition, the additional counts coming from the 4_1^+ excited state when the nucleus is at rest have to be taken into account. In our analysis this was achieved by subtracting the efficiency-corrected number of counts in the stopped component of the 660-keV line out of the efficiency-corrected number of counts in the stopped component of the 686-keV

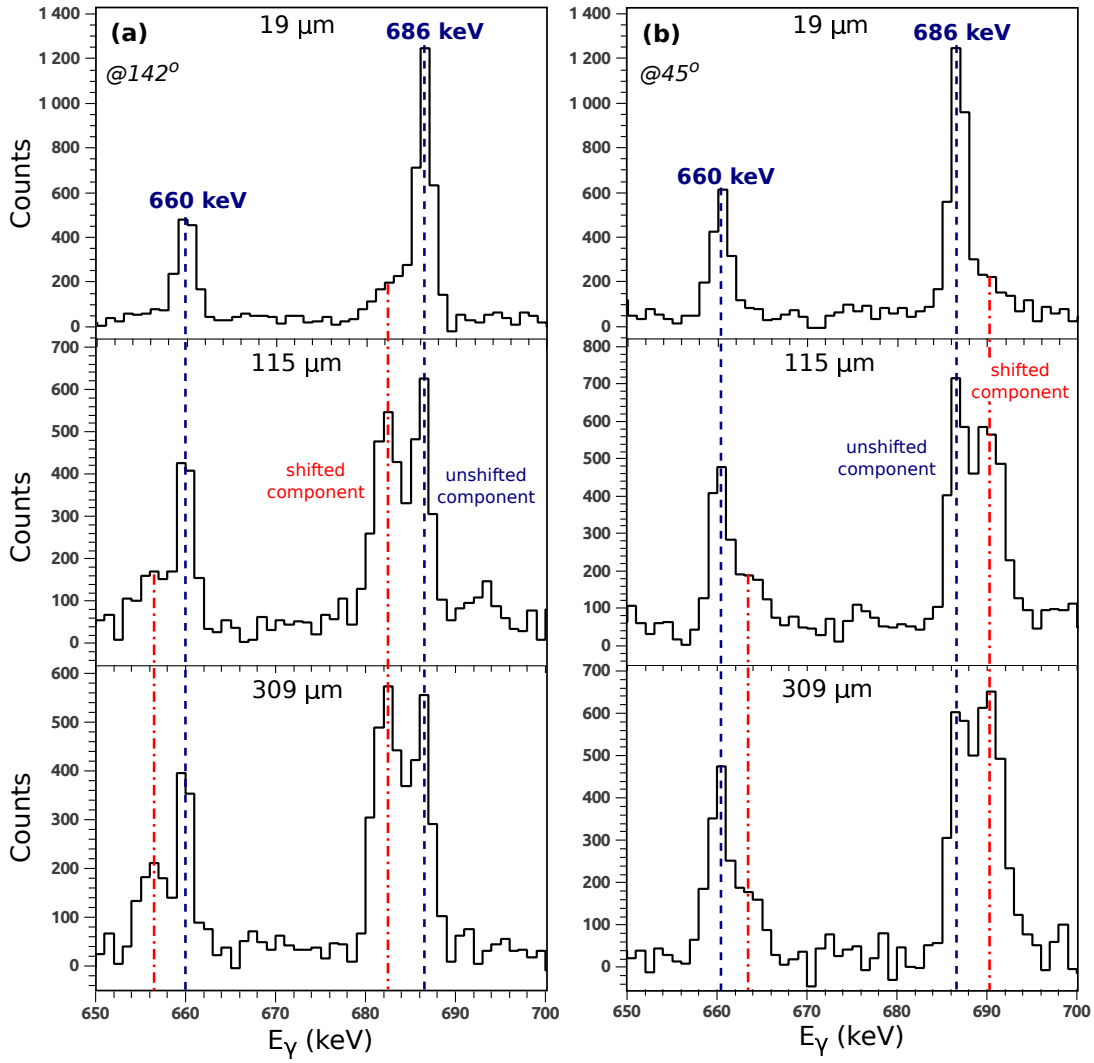

FIG. 2. (Color online) Examples of the evolution of the intensities of the Doppler-shifted peaks of the 686-keV ($2_1^+ \rightarrow 0_1^+$) and 660-keV ($4_1^+ \rightarrow 2_1^+$) transitions observed at backward angles (a) and at forward angles (b) for three different target-to-stopper distances. The dot-dashed lines (red) represent the positions of the Doppler-shifted peak and the dashed lines (blue) represent the unshifted peak positions.

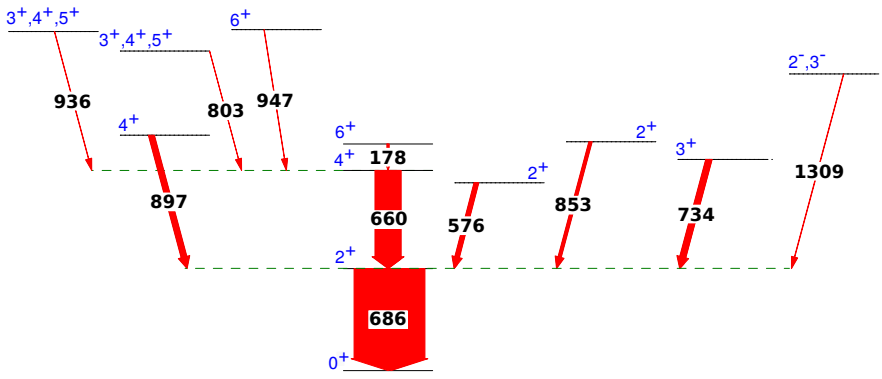

FIG. 3. (Color online) Partial level scheme of ^{208}Po showing the excited states, which feed the 2_1^+ and 4_1^+ states directly. The presented levels are based on the level scheme in our previous study, see Ref. [17]. The thicknesses of the arrows are proportional to the observed γ-ray intensities.

transition. The intensities of the shifted components of the 686-keV transition being directly determined from the particle-gated spectra should not be corrected by the feeding transitions. Hence, the intensities of the shifted and unshifted components of the 686-keV line being extracted with the procedure described above can be considered as effectively derived from γ-ray spectra in coincidence with the shifted components of all transitions directly feeding the state of interest. Therefore, they can be used to determine the lifetime of the 2_1^+ state of ^{208}Po. Since the evolution of the intensities of the shifted and unshifted components must be compared at each target-to-stopper distance in order to extract the lifetime of the level of interest, it is necessary that they refer to the same number of recoiling nuclei produced in the reaction. In our analysis the normalization factors for each distance were determined from the total number of counts of the I_{sh} and I_{un} components of the transition decaying the state of interest. In order to eliminate the influence of the lifetime of the 4_1^+ state, i.e. the evolution of the I_{sh} and I_{un} components of the 660-keV line, the normalization for the 686-keV transition was done after the correction of the intensities of its stopped components.

To proceed with the DDCM analysis the mean velocity of the recoiling nuclei $\langle v \rangle$ has to be known. This value was experimentally determined from the centroids of the shifted and the unshifted components of the 686-keV transition to be $\langle v \rangle$=0.75(7)%c. The DDCM analysis for the lifetime of the 2_1^+ state extracted with the procedure described above is presented in Fig. 4 for forward (a) and backward (b) angles. The average value between both results gives the value of 27(2) ps for the lifetime of the 2_1^+ state of ^{208}Po.

It has to be noted that the only assumption in the derivation of the result above which is not directly supported by experimental observations, is that the 3_1^+, 2_3^+ and $(2^-, 3^-)$ states are short-lived. In order to investigate the influence of these feeders on the lifetime of the 2_1^+ state further, we have also considered the alternative limit that they are long-lived and decay exclusively at rest. Then an additional reduction of the intensity of the stopped component of the 686-keV line has been done. The I_{un} component was reduced by 13% of the total intensity, which accounts for the intensities of the 734-, 853-, and 1309-keV transitions. This alternative approach reduces the obtained lifetime of the 2_1^+ to 15(2) ps. The average value of the two limits gives the value of 21 ps with a statistical uncertainty of 2 ps and an additional systematic uncertainty of 8 ps. As final value for the lifetime of the 2_1^+ we addopted the value of 21(8) ps. Taking into account the known electron conversion coefficient for the $2_1^+ \rightarrow 0_1^+$ transition of ^{208}Po [29] and the newly determined lifetime of the 2_1^+ state the absolute transition strength was calculated to be $B(E2; 2_1^+ \rightarrow 0_1^+)$=252(96) e^2fm^4=3.4(13) W.u.

The lifetime of the 4_1^+ state of ^{208}Po was determined in an analogous way to the analysis for measuring the lifetime of the 2_1^+ state. We have estimated that 29% of the feeding of the 4_1^+ state originates from the states depicted in Fig. 3 as follows: 23% from the 178-keV transition, 2% from the 803-keV transition, 2% from the 936-keV transition, and 2% from the 947-keV transition. Since the 660-keV ($4_1^+ \rightarrow 2_1^+$) transitions was not observed in coincidence with any transitions from higher-lying states or other unknown γ rays, the remaining 71% of the intensity of the 660-keV transition is considered to originate from a direct population of the 4_1^+ state. The half-life of the 6_1^+ of ^{208}Po is known to be 4.01(25) ns (cf. Ref. [29], this value is based on weighted average of values from [34–36]). Hence, the decay of this state contributes only to the stopped component of the 660-keV transition and the intensity of the unshifted 660-keV line had to be reduced by 23% of the total intensity. The lifetime of the $(3^+, 4^+, 5^+)$ state at excitation energy 2149 keV of the nucleus ^{208}Po was measured to be 0.47(5) ps [17], i.e. its contribution could be accepted only as fast feeding of the 4_1^+ state. The lifetimes of the remaining two states feeding directly the 4_1^+ state (see Fig. 3) are not known and cannot be determined from any of the available data sets. Similar to the analysis for the lifetime of the 2_1^+ state, we assumed both alternative limits. Firstly, we assumed that these feeders are short-lived and decay only in flight. Then we have considered that they decay only at rest and an additional reduction of the I_{un} component by 4% of the total intensity of the 660-keV line has been done. Fig. 5 represents the DDCM analysis for the lifetime of the 4_1^+ state for forward (a) and backward (b) angles when the feeders are considered to be short-lived. The average value between both results gives for the lifetime of the 4_1^+ the value of 133(17) ps. The alternative approach reduces the obtained lifetime of the 4_1^+ state to 111(16) ps. The average value of the two limits gives the value of 122 ps with a statistical uncertainty of 12 ps and an additional systematic uncertainty of 28 ps. For the final value of the 4_1^+ state of ^{208}Po we adopted the value of 122(30) ps. This value is in good agreement with the value of 125(35) ps which is extracted in [37]. Taking into account the known electron conversion coefficient for the $4_1^+ \rightarrow 2_1^+$ transition of ^{208}Po [29] we have calculated the absolute transition strength to be $B(E2; 4_1^+ \rightarrow 2_1^+)$=53(13) e^2fm^4=0.72(18) W.u.

IV. DISCUSSION

In order to study the low-energy states of ^{208}Po and in particular to investigate the structure of the yrast and yrar 2^+ states, we have performed shell-model calculations by considering ^{208}Pb as closed core and by using the model space spanned by the $2p_{3/2}$, $2p_{1/2}$, $1f_{7/2}$, $1f_{5/2}$, $0h_{9/2}$, $0i_{13/2}$ orbitals for the 2 protons valence particles and the 2 neutrons valence holes. Results are obtained by using the shell-model code KSHELL [38] and adopting the same theoretical framework of our previous study of ^{209}Po [39]. More precisely, the two-body matrix elements of the effective Hamiltonian are derived by means of the

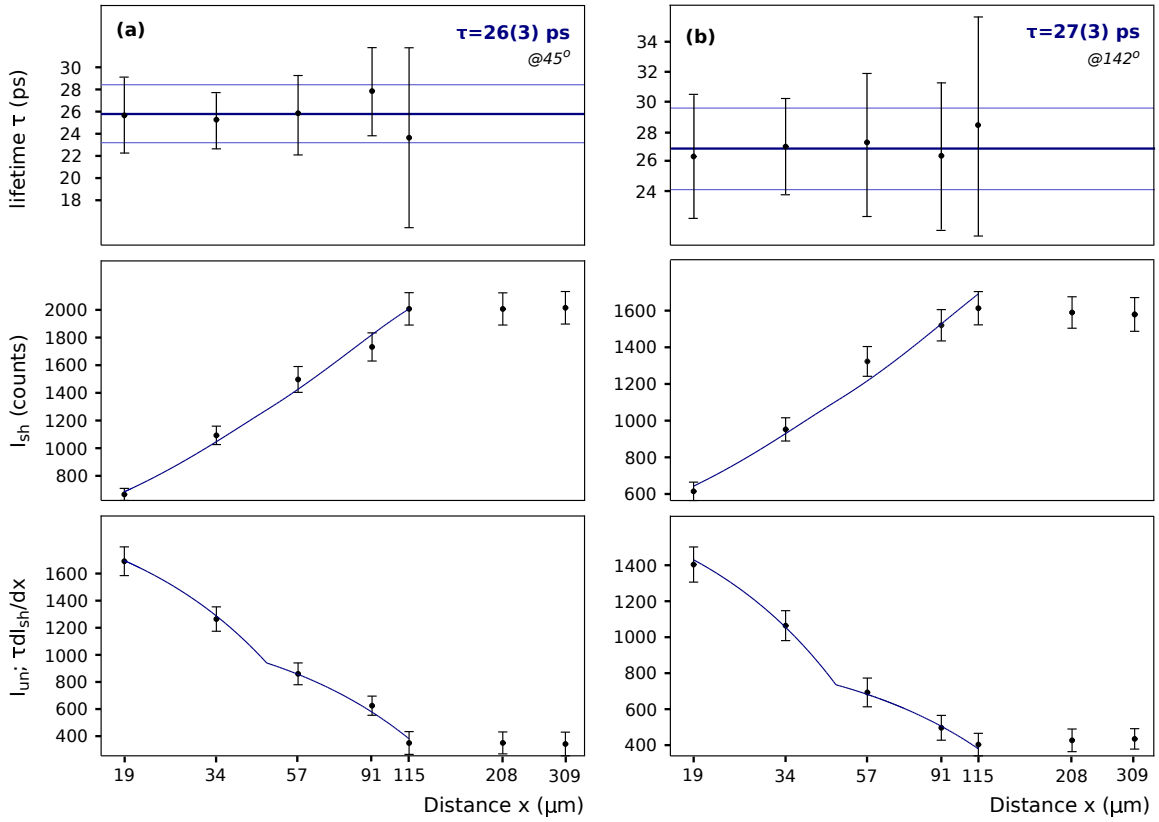

FIG. 4. (Color online) The lifetime of the 2_1^+ state of ^{208}Po determined at forward (a) and backward angles (b). In the middle panels the shifted intensities at different plunger distances are presented, in the region of sensitivity are fitted continuous curves to calculate the derivative. In the bottom panels, curves that represent the product between the time derivatives of the shifted intensities and the lifetime of the state of interest are compared with the experimental unshifted intensities. In the upper panels, the lifetimes corresponding to each distance in the region of sensitivity are extracted. The horizontal lines represent the weighted mean values.

$\hat{Q}$-box folded-diagram approach [40] starting from the realistic CD-Bonn nucleon-nucleon potential [41] renormalized by way of the $V_{\rm low-k}$ approach [42]. The Coulomb term for the proton-proton interaction is also included. The proton and neutron one-body component of the effective Hamiltonian are set by reference to the experimental spectrum of ^{209}Bi [43] and ^{207}Pb [44], respectively. More details are presented in [39]. In this paper we also briefly discussed our choice of the effective charges and effective gyromagnetic factors, whose values are reported here for completeness, $e_\pi = 1.5e$, $e_\nu = 0.92e$, $g_\pi^l = 1.2$, $g_\nu^l = -0.2$, $g_{\pi,\nu}^s = 0.7(g_{\pi,\nu}^s)_{bare}$.

The theoretical spectrum and electromagnetic properties, labeled as Calc1, are compared with the experimental data, labeled as Expt, in Tables I and II, respectively. The calculated excitation energies are in good agreement with the experimental values, discrepancies ranging from few keV to at most 100 keV. As concerns the $B(E2; 2_1^+ \rightarrow 0_1^+)$ and $B(E2; 4_1^+ \rightarrow 2_1^+)$ measured in the present experiment, we see that they are reasonably well reproduced by the theory, the calculated values falling just narrowly out of the experimental error range. This is also the case of the other electromagnetic properties reported in Table II, the only exceptions being transitions from the 8^+ and the second 2^+ states.

TABLE I. Calculated and experimental excitation energies (in keV) of ^{208}Po. See text for details.

J^π	Expt	Calc1	Calc2
0^+	0.0	0.0	0.0
2^+	687	769	850
2^+	1263	1163	1160
4^+	1347	1414	1366
6^+	1524	1520	1465
8^+	1528	1592	1538

The value of the $B(E2; 8_1^+ \rightarrow 6_1^+)$ is in fact underestimated by a factor 4. This result is in contrast with the nice agreement we find for the available measured moments of the 8^+ and 6^+ states in ^{208}Po as well as for the corresponding $E2$ transition rates in neighboring Po isotopes. The calculated $B(E2; 8^+ \rightarrow 6^+)$ from ^{204}Po to ^{210}Po are reported in Fig. 6 and compared with experimental data. Theoretical results follow approximately a straight line slightly increasing towards ligther Po isotopes, while experimental data show a large peak

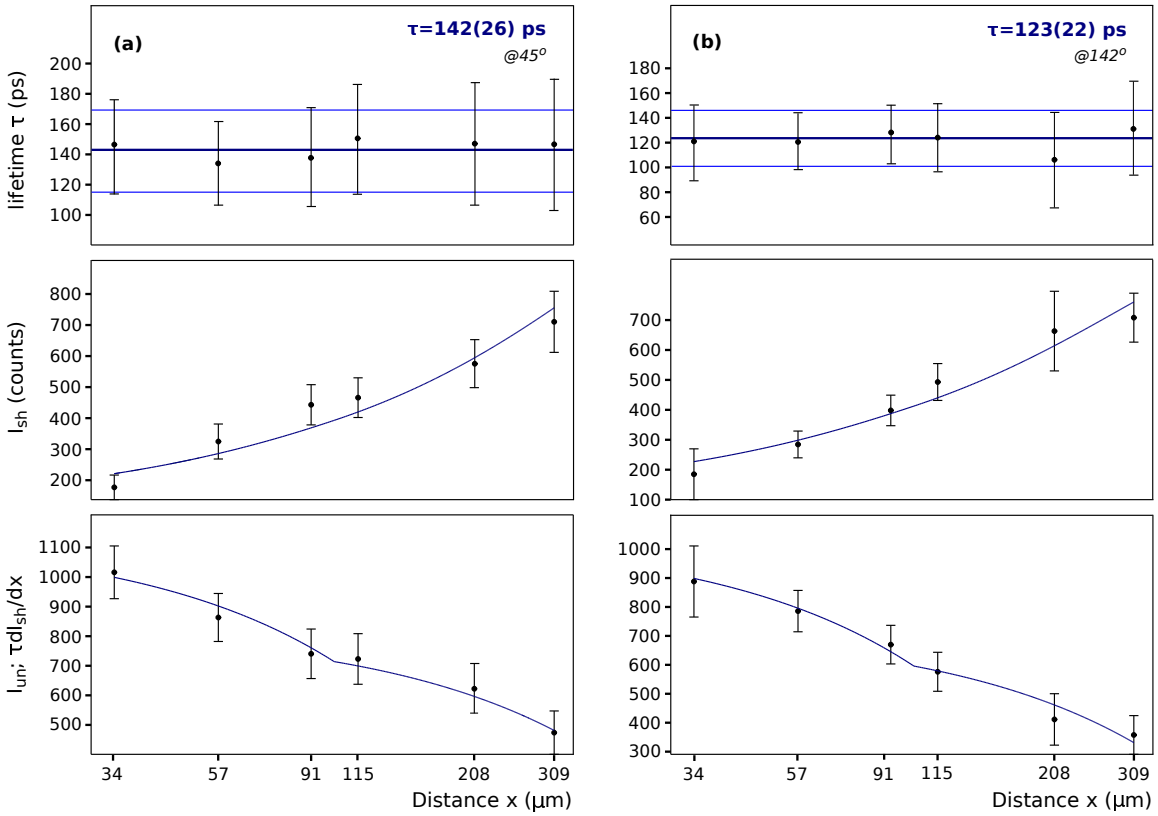

FIG. 5. (Color online) Analogous to Fig. 4 but for the lifetime of the 4_1^+ state of ^{208}Po.

TABLE II. Calculated and experimental reduced transition probabilities and moments in ^{208}Po. The $B(E2)$ values are given in $e^2\mathrm{fm}^4$, the $B(M1)$ in μ_N^2, the quadrupole moments in $e\mathrm{fm}^2$, and the magnetic moments μ are in μ_N. See text for details.

Quantity	Expt	Calc1	Calc2
$\mu(6^+)$	$+5.3(6)^{a}$	$+5.7$	$+5.7$
$\mu(8^+)$	$+7.37(5)^{a}$	$+7.66$	$+7.66$
$Q(8^+)$	$90(4)^{a}$	-76	-72
$B(E2;2_1^+\rightarrow 0_1^+)$	$252(96)^{b}$	388	420
$B(E2;4_1^+\rightarrow 2_1^+)$	$53(13)^{b}$	68	92
$B(E2;6_1^+\rightarrow 4_1^+)$	$410(29)^{a}$	350	327
$B(E2;8_1^+\rightarrow 6_1^+)$	$468(37)^{a}$	122	155
$B(E2;2_2^+\rightarrow 0_1^+)$	$85(13)^{c}$	163	154
$B(E2;2_2^+\rightarrow 2_1^+)$	$\leq 1158(139)^{c}$	16	5
$B(M1;2_2^+\rightarrow 2_1^+)$	$\geq 0.116(14)^{c}$	0.02	0.123
	$\leq 0.143(17)^{c}$		

[a] From Ref. [29].
[b] From the present work.
[c] From Ref. [17].

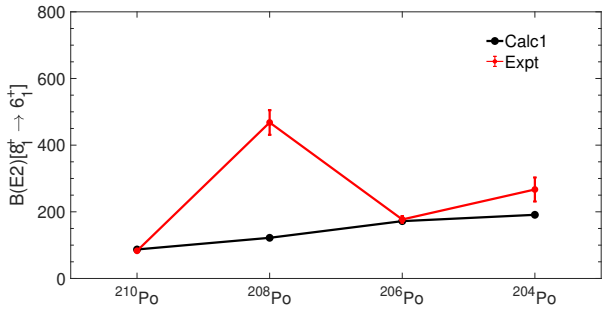

FIG. 6. Calculated and experimental $B(E2;8^+\rightarrow 6^+)$ (in $e^2\mathrm{fm}^4$) for Po isotopes from A=204 to 210. The experimental $B(E2)$ values are taken from Ref. [45] for ^{210}Po, from Ref. [29] for ^{208}Po, from Ref. [46] for ^{206}Po, and from Ref. [47] for ^{204}Po.

at ^{208}Po which implies a change in the nature of the involved states that is not predicted by theory.

A more detailed discussion is deserved to the 2_2^+ state. The observed $B(M1;2_2^+\rightarrow 2_1^+)$ and $B(E2;2_2^+\rightarrow 0_1^+)$ suggest that the 2_2^+ state could have a rather significant overlap with the one-phonon MSS, containing an equal amount of the two-proton and two-neutron components with opposite signs. In fact, experimental data show that the $B(E2;2_2^+\rightarrow 0_1^+)$ is a factor 3 smaller than the $B(E2;2_1^+\rightarrow 0_1^+)$, and the $2_2^+\rightarrow 2_1^+$ decay is dominated by the $M1$ transition [17]. This finding, however, is not confirmed by the calculations. In particular, the experimental $B(M1;2_2^+\rightarrow 2_1^+)$ is significantly underestimated by theory which may indicate some inaccuracies

in the structure we predict for the second 2^+ state.

To better clarify this point, we have written the 0_1^+, 2_1^+ and 2_2^+ wave functions in terms of two proton particles coupled to two neutron holes, namely we have used the $|^{210}\mathrm{Po}\rangle \otimes |^{206}\mathrm{Pb}\rangle$ basis states:

$$|^{208}\mathrm{Po}; 0_{gs}^+\rangle = 0.99|^{206}\mathrm{Pb}; 0_{gs}^+\rangle \otimes |^{210}\mathrm{Po}; 0_{gs}^+\rangle \quad (2)$$

$$|^{208}\mathrm{Po}; 2_1^+\rangle = 0.95|^{206}\mathrm{Pb}; 2_1^+\rangle \otimes |^{210}\mathrm{Po}; 0_{gs}^+\rangle + 0.25|^{206}\mathrm{Pb}; 0_{gs}^+\rangle \otimes |^{210}\mathrm{Po}; 2_1^+\rangle \quad (3)$$

$$|^{208}\mathrm{Po}; 2_2^+\rangle = 0.20|^{206}\mathrm{Pb}; 2_1^+\rangle \otimes |^{210}\mathrm{Po}; 0_{gs}^+\rangle - 0.62|^{206}\mathrm{Pb}; 0_{gs}^+\rangle \otimes |^{210}\mathrm{Po}; 2_1^+\rangle - 0.74|^{206}\mathrm{Pb}; 2_2^+\rangle \otimes |^{210}\mathrm{Po}; 0_{gs}^+\rangle. \quad (4)$$

where only components larger than 0.05 are reported.

The leading component of the 2_1^+ wave function is 90% $J_\nu = 2$, $J_\pi = 0$, while the probability of the $J_\nu = 0$, $J_\pi = 2$ component is smaller by a factor of about 14 (remaining terms covering $\sim 3\%$). This asymmetric superposition may be traced to the weakness of proton-neutron correlations in overcoming the energy difference between the two 2^+ yrast states in ^{206}Pb and ^{210}Po, which lie at 803 and 1181 keV, respectively.

This is also the case in ^{136}Te, with two valence protons and two valence neutrons with respect to ^{132}Sn, whose 2_1^+ wave function was found to be characterized by neutron dominance [21, 48, 49]. The 2_1^+ state of ^{132}Te can be instead identified with a FSS, with almost equal contributions from the neutron 2_1^+ excitation of ^{130}Sn and the proton 2_1^+ excitation of ^{134}Te [11].

As expected, the 2_2^+ state does not exhibit a mixed symmetry character. Its overlap with the one-phonon MSS is only 0.58 (34%), while the yrast 2^+ state, although showing an unbalanced proton-neutron character, is dominated by the FSS up to 73%. In fact, we find that two components arising from the 2_2^+ of ^{206}Pb and the 2_1^+ of ^{210}Po contribute with almost the same weight to the 2_2^+ wave function of ^{208}Po.

This result may point out to some inaccuracy in the matrix elements of our effective interaction, and in particular of the neutron-proton ones. A similar conclusion was reached for the off-diagonal matrix elements of the proton-neutron effective interaction in [39], where results of ^{209}Po were discussed.

On these bases, we have introduced empirical readjustments of the interaction matrix elements in the neutron-proton channel by applying monopole corrections [50, 51] to some peculiar observed properties of Po isotopes with $N < 126$ [52]. In particular, we have focused on the experimental energy of yrast 2^+ levels which remains almost constant going from ^{208}Po to ^{200}Po, the 8^+ and 6^+ states whose energies differ by only $\sim$10 keV giving an isomeric character to the 8^+ states [53], and the 2_2^+ behavior which shows a sudden decrease from 2290 keV in ^{210}Po to 1263 keV in ^{208}Po.

Our procedure leads to an increase in the absolute value of the $\pi 0h_{9/2}\nu 2p_{1/2}^{-1}$ monopole component by about 180 keV. More precisely, the two corresponding $J^\pi = 4^+$ and 5^+ matrix elements slightly decrease, going from 49 to -41 keV and 22 to -68 keV, respectively, The weakness of the $\pi 0h_{9/2}\nu 2p_{1/2}^{-1}$ interaction, which still persists after the modification, may be explained by the reduced overlap between the neutron orbital, with high principal quantum number and low angular momentum, and the proton $0h_{9/2}$ orbital, as it was pointed out in Ref. [53], where it was invoked to explain the validity of the seniority scheme in Pb neighboring with $Z > 82$ and $N < 126$.

The new results are shown in column Calc2 of Tables I and II. Note that for the calculation of the electromagnetic properties the same effective charges and gyromagnetic factors of Calc1 are employed. It can be seen that Calc2 produces, on the overall, negligible effects on the energy levels, moments and $E2$ transition rates with respect to Calc1. Actually, the $B(E2; 8^+ \to 6^+)$ is still underestimated by Calc2. However, an apparent improvement is obtained on the $B(M1; 2_2^+ \to 2_1^+)$ transition.

This improvement arises from a change in the structure of the 2^+ states, as can be seen in Eqs. 5, 6, and 7, where the 0_1^+, 2_1^+ and 2_2^+ wave functions resulting from the modified interaction are written in terms of the $|^{210}\mathrm{Po}\rangle \otimes |^{206}\mathrm{Pb}\rangle$ basis states.

$$|^{208}\mathrm{Po}; 0_{gs}^+\rangle = 0.99|^{206}\mathrm{Pb}; 0_{gs}^+\rangle \otimes |^{210}\mathrm{Po}; 0_{gs}^+\rangle \quad (5)$$

$$|^{208}\mathrm{Po}; 2_1^+\rangle = 0.93|^{206}\mathrm{Pb}; 2_1^+\rangle \otimes |^{210}\mathrm{Po}; 0_{gs}^+\rangle + 0.34|^{206}\mathrm{Pb}; 0_{gs}^+\rangle \otimes |^{210}\mathrm{Po}; 2_1^+\rangle \quad (6)$$

$$|^{208}\mathrm{Po}; 2_2^+\rangle = 0.33|^{206}\mathrm{Pb}; 2_1^+\rangle \otimes |^{210}\mathrm{Po}; 0_{gs}^+\rangle - 0.85|^{206}\mathrm{Pb}; 0_{gs}^+\rangle \otimes |^{210}\mathrm{Po}; 2_1^+\rangle - 0.33|^{206}\mathrm{Pb}; 2_2^+\rangle \otimes |^{210}\mathrm{Po}; 0_{gs}^+\rangle. \quad (7)$$

The modified interaction leaves unchanged the ground-state structure, while it significantly affects the 2_1^+ and

2_2^+ wave functions. As a matter of fact, the 2_1^+ state acquires a more symmetric superposition of the neutron and proton components, the $J_\nu = 0$, $J_\pi = 2$ and $J_\nu = 2$, $J_\pi = 0$ components differ now by a factor 7. A more significant change is produced in the 2_2^+ state, whose overlap with the one-phonon MSS becomes 0.84 (70%) with respect 0.56 (34%) of Calc1.

We can conclude this discussion by noting that although the original interaction, which does not contain empirical adjusted parameters, gives an overall good description of the low-energies states in ^{208}Po, it fails to describe properties that are very sensitive to the structure of wave functions. On the other hand, the slight overestimation of some B(E2) transitions shows also limits of the Calc2 calculations, which may be related to the choice of the effective charges as well as to the need of a fine tuning of interaction matrix elements in neutron-neutron and proton-proton channels. We would like to mention that the 4^+, 6^+, and 8^+ wave functions predicted by both Calc1 and Calc2 show a more simple structure as compared to the 2^+ states. In fact, they are all dominated by the configuration $\pi(0h_{9/2})^2\nu(2p_{1/2})^{-2}$ with a percentage of ~ 70 and 80% in Calc1 and Calc2, respectively.

V. SUMMARY

In the present study we have measured the lifetimes of the 2_1^+ and the 4_1^+ states of ^{208}Po by utilizing the RDDS method in an α-transfer reaction experiment. The extracted transition strengths together with the previously measured electromagnetic properties of the decay of the 2_2^+ state of ^{208}Po were compared to shell-model results obtained by using an effective interaction derived from the CD-Bonn nucleon-nucleon potential. The comparison indicates that the description of the properties of the 2_1^+ and the 2_2^+ states of ^{208}Po requires stronger neutron-proton correlations. We have therefore employed a modified interaction, whose $\pi 0h_{9/2}\nu 2p_{1/2}^{-1}$ monopole component was adjusted to reproduce some peculiar observed properties of Po isotopes with $N < 126$. The introduced change is sufficient to increase the isovector component of the 2_2^+ state leading to a good agreement with experimental data. This confirms the suggestion that this state is, at least, a fragment of the one-phonon mixed-symmetry state of ^{208}Po. The present study demonstrates the necessity to know the experimental properties of both isoscalar and isovector quadrupole states in order to find an appropriate microscopic description of these simplest collective excitations in even-even nuclei.

ACKNOWLEDGMENTS

D. Kocheva acknowledges the support by the Bulgarian Ministry of Education and Science under the National Research Program Young scientists and post-doctoral students. This work was supported by the BgNSF under grant KP-06-M28/1 (08/12/2018) and by DAAD under the partnership agreement between the University of Cologne and University of Sofia. We acknowledge the CINECA award under the ISCRA initiative code HP10B51E4M and through the INFN-CINECA agreement for the availability of high performance computing resources and support. G. De Gregorio acknowledges the support by the funding program VALERE of "Università degli Studi della Campania Luigi Vanvitelli". P.R.J. acknowledges the support by BMBF under grant number 05P19RDFN1. S.S.D. acknowledges the financial support of the BgNSF under contract No. KP-06-N38/1. M.S. and P.S. acknowledge financial support by the UK-STFC (grant ST/P005101/1).

[1] M. G. Mayer, Phys. Rev. **75**, 1969 (1949).
[2] O. Haxel, J. H. D. Jensen, H. E. Suess, Phys. Rev. **75**, 1766 (1949).
[3] F. Iachello, Phys. Rev. Lett. **53**, 1427 (1984).
[4] R. F. Casten, Phys. Lett. **B152**, 145 (1985).
[5] F. Iachello and A. Arima, *The Interacting Boson Model* (Oxford University Press, New York, 1990).
[6] N. Pietralla, P. von Brentano, A. F. Lisetskiy, Prog. Part. Nucl. Phys. **60**, 225 (2008) and the references therein.
[7] N. Pietralla, C. Fransen, D. Belic, P. von Brentano, C. Friessner, U. Kneissl, A. Linnemann, A. Nord, H. H. Pitz, T. Otsuka, I. Schneider, V. Werner, and I. Wiedenhöver, Phys. Rev. Lett. **83**, 1303 (1999).
[8] G. Rainovski, N. Pietralla, T. Ahn, C. J. Lister, R. V. F. Janssens, M. P. Carpenter, S. Zhu, and C. J. Barton, Phys. Rev. Lett. **96**, 122501 (2006).
[9] T. Ahn, L. Coquard, N. Pietralla, G. Rainovski, A. Costin, R. V. F. Janssens, C.J. Lister, M. Carpenter, S. Zhu, K. Heyde, Phys. Rev. Lett. **96**, 122501 (2006).
[10] L. Coquard, N. Pietralla, G. Rainovski, T. Ahn, L. Bettermann, M. P. Carpenter, R. V. F. Janssens, J. Leske, C. J. Lister, O. Möller, W. Rother, V. Werner, and S. Zhu, Phys. Rev. C **82**, 024317 (2010).
[11] M. Danchev, G. Rainovski, N. Pietralla, A. Gargano, A. Covello, C. Baktash, J. R. Beene, C. R. Bingham, A. Galindo-Uribarri, K. A. Gladnishki, C. J. Gross, V. Y. Ponomarev, D. C. Radford, L. L. Riedinger, M. Scheck, A. E. Stuchbery, J. Wambach, C. H. Yu, and N. V. Zamfir, Phys. Rev. C **84**, 061306(R) (2011).
[12] T. Ahn, G. Rainovski, N. Pietralla, L. Coquard, T. Moller, A. Costin, R. V. F. Janssens, C. J. Lister, M. P. Carpenter, and S. Zhu, Phys. Rev. C **86**, 014303 (2012).
[13] R. Kern , R. Zidarova, N. Pietralla, G. Rainovski, R. Stegmann, A. Blazhev, A. Boukhari, J. Cederkäll, J. G. Cubiss, M. Djongolov, C. Fransen, L. P. Gaffney, K. Gladnishki, E. Giannopoulos, H. Hess, J. Jolie, V. Karayonchev, L. Kaya, J. M. Keatings, D. Kocheva, Th. Kröll, O. Möller,1 G. G. ONeill, J. Pakarinen, P. Reiter, D. Rosiak, M. Scheck, J. Snall, P.-A. Söderstrm, P. Spag-

noletti, M. Stoyanova, S. Thiel, A. Vogt, N. Warr, A. Welker, V. Werner, J. Wiederhold, and H. De Witte, Phys. Rev. C **102**, 041304(R) (2020).
[14] D. Kocheva, G. Rainovski, J. Jolie, N. Pietralla, C. Stahl, P. Petkov, A. Blazhev, A. Hennig, A. Astier, Th. Braunroth, M. L. Cortés, A. Dewald, M. Djongolov, C. Fransen, K. Gladnishki, V. Karayonchev, J. Litzinger, C. Müller-Gatermann, M. Scheck, Ph. Scholz, R. Stegmann, P. Thöle, V. Werner, W. Witt, D. Wölk, and P. Van Isacker, Phys. Rev. C **93**, 011303(R) (2016).
[15] R. Stegmanna, C. Stahl, G. Rainovski, N. Pietralla, C. Stoyanov, M. P. Carpenter, R. V. F. Janssens, M. Lettmann, T. Möller, O. Möller, V. Werner, S. Zhu, Phys. Lett. **B770**, 77 (2017).
[16] R. Kern, R. Stegmann, N. Pietralla, G. Rainovski, M. P. Carpenter, R. V. F. Janssens, M. Lettmann, O. Möller, T. Möller, C. Stahl, V. Werner, and S. Zhu, Phys. Rev. C **99**, 011303(R) (2020).
[17] A. Yaneva, D. Kocheva, G. Rainovski, J. Jolie, N. Pietralla, A. Blazhev, A. Dewald, M. Djongolov, C. Fransen, K. A. Gladnishki, C. Henrich, I. Homm, K. E. Ide, P. R. John, D. Kalaydjieva, V. Karayonchev, R. Kern, J. Kleemann, Th. Kröll, C. Müller-Gatermann, M. Scheck, P. Spagnoletti, M. Stoyanova, V. Werner., Eur. Phys. J. A **56**, 246 (2020).
[18] N. Lo Iudice, V. Yu. Ponomarev, Ch. Stoyanov, A.V. Sushkov and V.V. Voronov, J. Phys. G., Nucl. Part. Phys. **39**, 043101 (2012).
[19] K. Heyde and J. Sau, Phys. ReV. C **33**, 1050 (1986).
[20] J. D. Holt, N. Pietralla, J. W. Holt, T. T. S. Kuo, and G. Rainovski, Phys. Rev. C **76**, 034325 (2007).
[21] N. Shimizu, T. Otsuka, T. Mizusaki, and M. Honma, Phys. Rev. C **70**, 054313 (2004).
[22] K. Sieja, G. Martinez-Pinedo, L. Coquard, and N. Pietralla, Phys. Rev. C **80**, 054311 (2009).
[23] D. Bianco, F. Andreozzi, N. Lo Iudice, A. Porrino, and F. Knapp, Phys. Rev. C **85**, 034332 (2012).
[24] D. Bianco, N. Lo Iudice, F. Andreozzi, A. Porrino, and F. Knapp, Phys. Rev. C **88**, 024303 (2013).
[25] D. Kocheva, G. Rainovski, J. Jolie, N. Pietralla, A. Blazhev, R. Altenkirch, S. Ansari, A. Astier, M. Bast, M. Beckers, Th. Braunroth, M. Cappellazzo, A. Dewald, F. Diel, M. Djongolov, C. Fransen, K. Gladnishki, A. Goldkuhle, A. Hennig, V. Karayonchev, J. M. Keatings, E. Kluge, Th. Kröll, J. Litzinger, K. Moschner, C. Müller-Gatermann, P. Petkov, M. Scheck, Ph. Scholz, T. Schmidt, P. Spagnoletti, C. Stahl, R. Stegmann, A. Stolz, A. Vogt, N. Warr, V. Werner, D. Wölk, J. C. Zamora, K. O. Zell, V. Yu. Ponomarev, and P. Van Isacker, Phys. Rev. C **96**, 044305 (2017).
[26] T. K. Alexander and J. S. Forster, Adv. Nucl. Phys. **10**, 197 (1978).
[27] A. Z. Schwarzschild, E. K. Warburton, Ann. Rev. Nucl. Sci. **18**, 265 (1968).
[28] A. Dewald, O. Möller, and P. Petkov, Prog. Part. Nucl. Phys. **67**, 786 (2012).
[29] M. J. Martin, Nucl. Data Sheets **108**, 1583 (2007).
[30] A. Dewald, S. Harissopulos and P. von Brentano, Z. Phys. A **334**, 163 (1989).
[31] G. Böhm, A. Dewald, P. Petkov and P. von Brentano, Nucl. Inst. Meth. A **329**, 248 (1993).
[32] B. Saha, *Bestimmung der Lebensdauern kollektiver Kernanregungen in ^{124}Xe und Entwicklung von entsprechender Analysesoftware*, PhD thesis, Universität zu Köln (2004).
[33] A. Astier, P. Petkov, M.-G. Porquet, D. S. Delion, and P. Schuck, Phys. Rev. Lett. **104**, 042701 (2010).
[34] William J. Treytl, Earl K.Hyde, Toshimitsu Yamazaki, Nucl. Phys. A **177**, 481-508 (1968).
[35] O.Häusser et.al., Nucl. Phys. A **273**, 253-268 (1976).
[36] A. R. Poletti et.al., Nucl. Phys. A **615**, 95-116 (1997).
[37] M. Stoyanova, V. Karayonchev, G. Rainovski, J. Jolie, N. Pietralla, A. Blazhev, A. Dewald, M. Djongolov, A. Esmaylzadeh, C. Fransen, J. Garbe, L. Gerhard, K. A. Gladnishki, K. Ide, P. R. John, R. Kern, J. Kleemann, D. Kocheva, Th. Kröll, C. Müller-Gatermann, J.-M. Régis, P. Spagnoletti, V. Werner and A. Yaneva, Jour. of Phys.: Conf. Ser. **1555** 012019 (2020).
[38] N. Shimizu, T. Mizusaki, T. Utsuno, and Y. Tsunoda, Comput. Phys. Commun. **244**, 372 (2019).
[39] V. Karayonchev, M. Stoyanova, G. Rainovski, J. Jolie, A. Blazhev, M. Djongolov, A. Esmaylzadeh, K. Gladnishki, D. Kocheva, L. Kornwebel, J. -M. Régis, G. De Gregorio, and A. Gargano, Phys. Rev. C **103**, 044309 (2021).
[40] L. Coraggio, A. Covello, A. Gargano et al., Ann. Phys. (NY) **327**, 2125 (2012).
[41] R. Machleidt, Phys. Rev. C **63**, 024001 (2001).
[42] S. Bogner, T. T. S. Kuo, L. Coraggio, A. Covello, and N. Itaco, Phys. Rev. C **65**, 051301(R) (2002).
[43] J. Chen, F.G. Kondev, Nuclear Data Sheets **126**, 373 (2015).
[44] F. G. Kondev, S. Lalkovski, Nuclear Data Sheets **112**, 707 (2011).
[45] M. Shamsuzzoha Basunia, Nucl. Data Sheets **121**, 561 (2014).
[46] F. G. Kondev, Nucl. Data Sheets **109**, 1527 (2008).
[47] C. J. Chiara and F. G. Kondev, Nucl. Data Sheets **111**, 141 (2010).
[48] D. C. Radford, C. Baktash, J. R. Beene, B. Fuentes, A.Galindo-Uribarri, C. J. Gross, P. A. Hausladen, T. A. Lewis, P. E. Mueller, E. Padilla, D. Shapira, D. W. Stracener, C.-H. Yu, C. J. Barton, M. A. Caprio, L. Coraggio, A. Covello, A. Gargano, D. J. Hartley, and N. V. Zamfir, Phys. Rev. Lett. **88** 222501 (2002).
[49] D. C. Radford, C. Baktash, J. R. Beene, B. Fuentes, A.Galindo-Uribarri, C. J. Gross, P. A. Hausladen, T. A. Lewis, P.E. Mueller, E. Padilla, D. Shapira, D. W. Stracener, C.-H. Yu, C. J. Barton, M. A. Caprio, L. Coraggio, A. Covello, A. Gargano, D. J. Hartley, and N. V. Zamfir, in *Proceedings of theInternational Symposium on Frontiers of Collective Motions* ,edited by H. Sagawa and H. Iwasaki (World Scientific, Singapore, 2003), p. 318.
[50] J. Duflo and A. P. Zuker, Phys.Rev. C **59**, R2347(R) (1999).
[51] A. P. Zuker, Phys. Rev. Lett. **90**, 042502 (2003).
[52] Data extracted using the NNDC On-line Data Service from the ENSDF database, file revised as of December 12, 2020., URL https://www.nndc.bnl.gov/ensdf.
[53] J. J. Ressler, C. W. Beausang, et *al.*, Phys.Rev. C **69**, 034331 (2004).